Histological and Immunohistochemical Study on the Possible Ameliorative Effect of Propolis in Experimental Adenine -Induced Chronic Kidney Disease of Adult Male Albino Rats

Original Article

Nadia El- Akabawy[1], Heba M. Elnegris[1,2], Abeer A. Abdelrahman[3] and Ebtehal Z. Hassan[1]

Department of Medical Histology and Cell Biology, Faculty of Medicine, [1]Zagazig University, [2]Badr University, Egypt

[3]Department of Biochemistry and Molecular Biology, Faculty of Medicine, Zagazig University, Egypt

ABSTRACT

Introduction: Chronic kidney disease (CKD) is a major public health problem worldwide. The pathophysiological basis of the disease and its complication include inflammation and oxidative stress, which are similar in humans and animals. In this study, we seek to develop new therapeutic modalities for CKD.

Aim of the Work: This study aimed to investigate the ameliorative effects of propolis (Prop) in experimental adenine (AD) induced model of CKD.

Materials and Methods: Twenty-four Sprague-Dawley rats were allocated into four equal groups as following: control group, AD group received adenine 200 mg/kg/day orally for 28 days to induce CKD, (Recovery group) received AD as previous group then left untreated for another 14 days. (Prop treated group) received Propolis 100 mg/kg b.w/ day in addition to AD for 28 days. At the end of experiment, body weight and kidney weight were estimated for all groups. In addition, blood samples were obtained to estimate serum urea and creatinine. kidney function tests, oxidative stress markers and levels of miRNA-21-5p, miRNA-103a-3p, miRNA-192-5p were evaluated. Histopathological measurement of renal tissues and immunohistochemical staining for tumor necrosis factor α were performed.

Results: Propolis significantly decreased body weight loss and urine volume and improved renal hemodynamic changes caused by AD. In addition, it significantly improved kidney function tests and biomarkers of oxidative stress. A significant decrease of P53 immunohistochemical demonstration was documented. It also apparently reduced histopathological changes induced by AD.

Conclusion: Propolis may play a promising role in renal tissue structural and functional preservation in AD induced chronic kidney disease, making it a desirable supplement.

INTRODUCTION

Chronic kidney disease (CKD) is an alarming global health burden. Its complications lead to elevated disability and mortality rates. It is a long-term disease load to the healthcare system with a vast social cost equally in developed and developing countries. About 8 hundred million individuals all over the world suffer from some degree of CKD[1].

All available therapeutic interventions for CKD are based on preventing the deterioration of the condition and keeping the blood glucose and blood pressure normal[2].

Consequently, new treatment approval is extremely needed either for stoppage the progression of the disease or improvement of the kidney function[3]. The Adenine -induced model of CKD is a very helpful and commonly used approach helping to understand the physiological, biochemical, and histopathological backgrounds of the disease, testing the different useful therapeutic approaches[4].

Inflammatory reactions, oxidative stress and apoptotic changes explain many of the pathophysiological processes of CKD and its complications. Both humans and experimental animals with CKD express a high profile of cytokines and inflammatory arbiters e.g., C reactive protein and tumor necrosis factor α. Additionally; there is a spike in oxidative stress and nitrosative indicators[5].

Recently, there is a rising concern about ancient and traditional folk medicine. One of its branches, called, apitherapy that targets treating diseases with all bee

products. Propolis is a product made from resins and plant ooze. It differs chemically according to geographic climate, surrounding flora, and picking time. It is used by bees as a natural guard to protect hives from invaders[6].

Propolis has many biological and chemical qualifications making it usable medically by many generations among decades[7]. It has been shown that propolis has many microbicidal, antioxidant, anticancer, antiviral, vasodilator, anti-ulcer, and anti-inflammatory traits[8].

Propolis is rich in bioactive components e.g., quercetin, trans-Cinnamic acid, artepillin C, caffeic acid phenethyl ester (CAPE), aromadendrin, and p-coumaric acid explaining its valuable unique pharmacological properties[9].

The aim of this work is to check the potential ameliorative impact of Propolis supplementation on the histological, ultrastructural, and biochemical changes in the kidney due to adenine induced CKD and to illuminate the probable underlying technicality.

MATERIAL AND METHODS

Animals

An entirety of 24 male rats (Sprague-Dawley 13-16 weeks) weighing initially (200–240 g). We got them from the Animal House, Faculty of Medicine at Zagazig University. They permitted free entrance to water plus a marketable standard chow diet containing (10-mm pellets bites, sniff® R/M-H-, -V1534-0) comprising 0.75% -phosphorus, 1. 2% -calcium, 0.35% -magnesium, 20% -simple protein and 2.5 IU/g- vitamin D,33.5%- raw fat, 35.5%- starch, and 4.5%- sugar. All experiments were agreeable rendering to protocols permitted by the local experimental ethics committee responsible for animal-research in Faculty of Medicine- Zagazig University and agreed with the the Care and Use Guide for Laboratory Animals.

(ZU-IACUC/3/F/190/2023).

Chemicals

We purchased adenine from Sigma company (St. Louis, MO, USA).

Propolis was obtained in the form of sticky concentrate from Emtinan Company- Egypt.

The antibody for P53 was purchased from (Vectastain Lab-Inc., Burlingame-CA- USA).

Study design

We devided rats at random manner into four groups, each group containing (6 rats) and were handled as follows:

Group I (control- group): we subdivided experimental rats into three subgroups (2 rats each):

- Group I A: animals supplied with water and food freely without receiving any treatment.

- Group I B (Vehicle control): animals were given normal saline orally at 9 a.m. for 28- consecutive days.

- Group I C (Positive control): rats took Propolis at an amount of 100mg/kg b.w/ day[10]. Every rat got 1 ml distilled water including 10 mg Propolis by orally at 12 p.m. for 28 days.

Group II (AD treated group): were given a single dose of AD 200 mg/kg/day dispersed with normal saline through oral route at 9 a.m. for 28 consecutive days to provoke CKD[5].

Group III (Recovery group): rats were treated with AD 200 mg/kg dispersed with normal saline through oral route at 9 a.m. for 28 consecutive days therefore were held untreated for extra 14 days[11].

Group IV (Propolis- treated group): rats got together Propolis 100 mg/kg b.w/ day at 12 p.m. once besides AD 200 mg/kg dispersed with normal saline orally at 9 a.m. daily, by oral gavage for 28 days[10]. The body weight for all animals was measured initially and at the end of the experiment. On the 29th day of the experiment for Group I, II and IV and on 43th day of the experiment for group III all animals were sacrificed.

At the end of the experiment the animals were put individually in metabolic cage sides for 24h to collect urine, and then they were kept in a transparent acrylic jar with (2 ml) of ether inhalation for about 2 min to be anesthetized[12]. and blood was collected. The samples of blood were exposed for centrifugation at 3000 rpm for 20 min. The serum element of blood was taken away and conserved at -80°C until processed. It used for estimation of urea and creatinine by colorimetrical techniques (Diamond Diagnostics-Egypt)[13].

Then a median incision laparotomy was done to expose the right and left kidneys and it was removed for each rat, smirched on filter paper firstly then weighed. The right kidney homogenate was kept in ice-cold phosphate buffer saline and then centrifuged at 3000 rpm for 15 min, then we preserved the supernatant at -20°C to be used[14].

We followed EGTI system for scoring and evaluating the extent of histological injuries[15]. This order involves histological injury in 4 separate constituents: glomerular, tubular, endothelial and interstitial (Table 1).

Table 1: The endothelial glomerular tubular interstitial (EGTI) histology scoring system.

Tissue type	Damage	Score
Tubular	No damage	0
	Loss of Brush Border (BB) in less than 25% of tubular cells. Integrity of basal membrane	1
	Loss of BB in more than 25% of tubular cell, thickened basal membrane	2
	(Plus) Inflammation, necrosis up to 60% of tubular cell	3
	(Plus) Necrosis in more than 60% of tubular cells	4
Endothelial	No damage	0
	Endothelial swelling	1
	Endothelial disruption	2
	Endothelial loss	3
Glomerular	No damage	0
	Thickening of Bowman capsule	1
	Retraction of glomerular tuft	2
	Glomerular fibrosis	3
Interstitial	No damage	0
	Inflammation, hemorrhage in less than 25% of tissue	1
	(Plus) necrosis in less than 25% of tissue	2
	Necrosis up to 60%	3
	Necrosis more than 60%	4

Biochemical study

Kidney function assessment

Estimation of the concentrations of seum urea and creatinine were done by colorimetrical techniques (Diamond Diagnostics, Egypt).

Biochemical analysis of tissues homogenate

Tissue level estimation of tumor necrosis factor-alpha (TNF-α) using ELISA kits Purchased from Ray Biotech (Georgia, USA). Estimation of Tissue levels of vascular endothelial growth factor-A (VEGF-A) using ELISA approach (R&D Systems- MN, USA). All the techniques were completed corresponding to the industrialist's directions[16].

To detect the oxidative stress status in kidney homogenate, we estimated oxidative stress markers. Superoxide dismutase (SOD), malondialdehyde (MDA) Lipid peroxidation derivative, glutathione perioxidase (GSH-Px) and catalase (CAT) using marketable available colorimetric kits (Biodiagnostic, Giza, Egypt) according to manufacturer's instructions[17].

We assesed Malondialdehyde (MDA) as a marker for lipid peroxidation by calorimetric method in kidney homogenate using a (Biodiagnostic, Egypt; Catalog Number: MD 25 29) kit. That method involves reaction of MDA with thiobarbituric acid (TBA) in presence of an acidic PH to give a pink product. That can be measured at 534 nm colorimetrically for absorbence[18].

miRNA isolation and reverse transcription

We isolated miRNA using mirVanaTM PARISTM extraction Kit, ambion- USA. We mixed 300 µL of Binding Buffer solution with serum sample by vortexing then added 300 µL 70% ethanol. 50 ul of the RNase free sterile water provided with the kit was used for miRNA elution. The resultant purified miRNA was kept at −70°C. to detect quality of isolated RNA we used Nanodrop® spectrophotometer to measure the absorbance at 260 nm, 280 nm, and 230 nm respectivly.

Assessment of expression levels of miRNA-21-5p, miRNA-103a-3p, miRNA-192-5p, in serum

To assess the quantity of the amplified miRNA, we used the TaqMan ® MicroRNA Assays reverse transcription Kit (Applied Biosystems). TaqMan ® MicroRNA Assay concurrently with the TaqMan ® Universal PCR Master Mix were used for amplification of cDNA specimens. RT reactions was done in (15 µL) including 7 µL of master mix, 5 µL RNA specimen and 3 µL primer. RT was run in a thermocycler for 30 min at 16°C., 42°C for 30 min, 85°C for 5 min. PCR was performed at 50°C for 2 min through the stage of enzyme initiation at 94°C for 10 min, then followed by 40 cycles of denaturation at 95°C for 15 s, annealing and expansion at 60°C for 60 s. In this work we standardized data using endogenous control gene snRNA (U6).

Data analysis

ΔCt was calculated by deducting Ct standards of the endogenous control (snRNA U6) from the Ct standards of the specimen miRNA. The ΔΔCT is estimated via deducting ΔCT of an tested specimen from a control. Fold change (FC) is calculated by 2-ΔΔCt method for relative expression[19].

Histological study

The left kidney was immediately taken, carefully dissected into halves, the 1st half was immediately fixed in formol saline 10% concentration, then processed into paraffin blocks. Thin renal sections at 4-5 µm thickness were stained with:

1. Hematoxylin & Eosin (H &E) stain for basic histological analysis[20].

2. Mallory trichrome (M.T) for detecting collagen fibers and assessing degrees of fibrosis[21].

3. Immunohistochemistry stain for p53 protein to evaluate the apoptosis:

Immunohistochemical detection kits for P53 standard avidin-biotin- peroxidase complex (ABC). We deparaffinized the 4 mm tissue sections, rehydrated them then incubated the slides in fresh H_2O_2 0.3%, prepared in methanol, at room temperature for 30 min. Graded

ethanol series rehydrated the sections, then heated up for 10 minutes via microwave preadjusted at 90° C for antigen retrieval. Tissue sections were directly cooled down to 30° C. Normal horse serum was added to all slides for 30 min, then slides were left overnight incubated with Mabs at 4° C. Phosphate buffered saline (PBS) washed the excess Mabs before incubation with secondary antibody. Skin was used as positive control and by omitting the primary antibody, negative control was obtained. The sections were counterstained with hematoxylin stain. Brown discoloration was considered the positive reaction[22].

Ultrastructural study

Tissue samples of the 2nd half of left kidney were immediately preserved at 4°C in glutaraldehyde buffered with 0.1 mol/L PBS at pH 7.4 at concentration of 3% for 3 hours. Specimens were fixed again in in the same buffer but with osmium tetroxide at 1 % concentration for another 2 hours at the same temperature. Ascending grades of alcohol dehydrated the tissue before being embedded in epoxy resin. Ultrathin renal sections were stained with lead citrate and uranyl acetate to be examined and photographed using a transmission electron microscope (JEOL, JEM-2100, Tokyo, Japan) at the Faculty of Medicine, Al Azhar Baneen University, Cairo, Egypt[23].

Morphometrical study

For quantitative estimation, ten various single fields from each section were weighted using (Leica Qwin 500, Cambridge, UK) in the image analysis unit at the Pathology Department, Faculty of Dentistry, Cairo University. The determined readings were estimated using the software (Image J 1.5.3). At (X 400), different H&E, MT and immunohistochemical prepared sections were evaluated for following parameters[24]:

- Measurement of Bowman's space width.
- Estimation of renal corpuscle diameter.
- Diameter of proximal convoluted tubule lumen.
- Diameter of distal convoluted tubule lumen.
- Area% of Mallory's Trichrome stained collagen fibers.
- Optical density for P53 positive stained areas.

Statistical analysis

All numeric biochemical and morphometrical found results are conveyed as mean± standard deviation of mean (M± SDM). We utilized one-way analysis of variance (ANOVA) to compare results, followed by Tukey posttest. The degree of significance was considered when *P-values* less than o.o5. SPSS program was used to perform the analysis (IBM compatible computer, version 17, SPSS Inc., Chicago, Illinois, USA)[25].

RESULTS

We considered all control subgroups as one group, as their results were similar.

Mortality rate

All through the study duration of different groups, no recorded animal loss.

Biochemical results

Body weight and kidney function results

All of the animals were healthy at the start of the trial. It showed normal physical activity and food intake. During the study, animals in the AD group displayed symptoms of a severe illness throughout the research, including a drastic drop in activity level, severe weakness, and a severe reduction in food intake. Animals of control and (AD+ Prop) groups were kept in good health all through the experiment. On the other hand, rats of recovery group showed the same picture as AD group during the 1st 28 days, its physical activity began to improve during the 2nd half of the study, but it never come back to the normal physical condition.

In the (AD+ Prop) group compared to the AD group, a statistically significant increase in body weight was seen ($p \leq 0.05$). There is not a noticeable distinction between the AD and recovery groups.

In comparison to the control group, the adenine and recovery groups both displayed a significantly lower body weight ($p \leq 0.05$). In the (AD+ Prop) group compared to the AD group, a statistically significant increase in body weight was seen ($p\ 0.05$). There is not a significant distinction between the AD and recovery groups (Table 2).

Regarding kidney function tests, as shown in (Table 2), it was discovered that both AD and recovery groups had significantly higher blood levels of urea and creatinine, as well as urine volume, as compared to the control and (AD+ Prop) groups ($p \leq 0.001$). Additionally, (The difference between the control and (AD+ Prop) groups was not statistically significant ($p \geq 0.05$).

Serum miRNA-21-5p, miRNA-103a-3p, miRNA-192-5p exepression levels

The expression of miRNA-21-5p, miRNA-103a-3p, and miRNA-192-5p was found to be significantly higher in the AD group than in the control group, according to our research. The values decreased in recovery group but without return back to normal values. In propolis treated group our results showed marked significant decrease in miRNA exepression levels compared to AD group. That clears the role of propolis in improvement of levels of miRNA exepression in studied groups (Table 3).

Lipid peroxidation and antioxidant enzymes

Regarding to renal tissue oxidative stress markers, there was significant decline of antioxidant enzymes GSH-px, SOD, CAT ($p \leq 0.001$) in AD group in comparison to both control and (AD+ Prop) groups. Their levels were gradually increased in recovery group but without significance. Propolis treated group showed significant increase in antioxidant enzyme levels nearly close to

normal levels of control group. Furthermore, the results showed no obvious difference between the control and (AD+ Prop) groups (Table 4).

The amount of MDA in the renal tissue increased significantly ($p ≤0.001$) after adenine delivery. While Propolis therapy prevented the oxidative damage demonstrated by the significantly substantial ($p≤0.001$) drop in MDA (Table 4).

Comparing the AD treatment and recovery groups to the control group, there was a highly significant rise ($p ≤0.001$) in MPO concurrent with renal leukocytic infiltration. The proinflammatory cytokine TNF-α and the angiogenic factor VEGF-A both showed a greatly significant increase ($p≤0.001$) in comparison to the control group, indicating an increase in the renal inflammatory responses. In contrast to both the AD and recovery groups, propolis therapy has a positive effect on standardizing all these parameters to control levels (Table 5).

Histological results

Light microscopic findings

Sections of the control group (group I) stained with hematoxylin and eosin showed that the renal cortical tissue included renal Malpighian corpuscles made up of rounded glomerular tufts of capillaries surrounded by membranes lined with simple squamous epithelium with a narrow Bowman's space. Proximal convoluted tubules appeared with a simple cuboidal epithelial lining, deep acidophilic cytoplasm, rounded nuclei at the base, and brush borders surrounding a narrow lumen. Distal convoluted tubules had a broader lumen, cuboidal cell lining with less-clear brush borders and centrally rounded nuclei, as well as less-acidophilic cytoplasm. (Figure 1A).

Renal cortical tissue sections of AD treated group (group II) manifested with significant massive histological changes. The glomeruli appeared shrunken and atrophied with widening of Bowman's space (Figures 1B,C). Kidney tubules appeared widened (Figures 1B,C) with hydropic degeneration of epithelial lining (Figures 1B,C). Some glomerular capillaries lined with small darkly stained nuclei (Figure 1C). Renal cortical interstitial tissue showed areas of acidophilic exudate (Figure 1B), congestion (Figure 1C) and cellular infiltration (Figure 1D).

Examination of renal cortical tissue of the recovery group (group III) revealed the persistence of most of the previous changes in the form of shrunken glomeruli with broadening of Bowman's space. Renal tubules were expanded with hydropic degeneration of its epithelial lining. Renal interstitial tissue cellular infiltration was observed (Figure 1E).

Preserved renal cortical tissue was displayed in (AD+ Prop) group (group IV). Renal glomeruli and renal tubules appeared more or less normal (Figure 1F).

Mallory's trichrome stain: (Histogram 3)

Mallory's trichrome stained sections of the renal

cortical tissue from control group I displayed very few fibers of collagen in renal interstitial tissue, as in between glomerular tuft of capillaries.

(Figure 2A) Though, the collagen fibers amount within renal cortical interstitial tissue and in renal glomerular capillaries were extremely significantly increased ($p≤0.001$) in AD treated group (Figure 2B). However, the amount of collagen fibers in the recovery group was remained substantially higher ($p ≤0.001$) (Figure 2C). Limited significant amount of collagen fibers were identified in renal cortical interstitial tissue and in glomerular capillaries in (AD+ Prop) group (Figure 2D).

Mmunohistochemical staining of P53: (Histogram 4)

Regarding P53 immune expression, control group's renal cortical tissue exhibited a negative immune reaction to the P53 in renal glomerular epithelial cell cytoplasm. and kidney tubular cytoplasm (Figure 3A). The Adenine treated group showed intense positive immune expression of P53 in the form of brown coloration of glomerular and tubular epithelial cell cytoplasm (Figure 3B). However, the recovery group revealed moderate positive immune expression of P53 in glomerular and tubular epithelial cell cytoplasm (Figure 3C). On the other hand, (AD+ Prop) group showed minimal positive immune expression of P53 in glomerular and tubular epithelial cell cytoplasm (Figure 3D).

Transmission electron microscopic findings

Renal cortical tissue of control group (group I) displayed podocytes with euchromatic nuclei lining renal glomeruli. They have glomerular blood capillaries that are wrapped by primary and secondary interdigitating secondary foot processes that are lined with fenestrated endothelium. The glomerular capillaries' basement membrane was uniform, smooth, and continuous (Figure 4A).

Cuboidal epithelial cells with a central euchromatic nucleus line the proximal convoluted tubule, resting on well-defined basement membrane. The epithelial lining has long narrow luminal microvilli. The cytoplasm exhibited many longitudinal located mitochondria, lysosomes, and vesicles (Figure 4B).

The distal convoluted tubule has cuboidal epithelial lining with central euchromatic nuclei resting on well-defined basement membrane. The epithelium has sparse luminal microvilli and many basal infoldings. The cytoplasm is full of mitochondria, ribosomes, and some vesicles. Tight junctions were seen joined the plasmalemma of adjacent cells (Figure 4C).

On the other hand, the glomerular basement membrane exhibited uneven thickening in the renal cortical tissue of the AD-treated group. The nuclei and wide fused secondary foot processes of the podocytes were visible (Figure 5A).

Proximal convoluted tubules had darkly stained nuclei with irregular nuclear envelop. The cytoplasm had distorted and disoriented mitochondria, many vacuoles

and lysosomes. The basement membranes were thick and the microvilli were irregular (Figure 5B). Some proximal convoluted tubules appeared with heterochromatic nuclei and exhibited electron dense bodies in their cytoplasm and few short basal infoldings (Figure 5C).

Distal convoluted tubules lining epithelium had small darkly stained nuclei. The cytoplasm had many vacuoles. The epithelium lost its basement membrane and was replaced by many collagen fibers and the interstitial cell nuclei were noticed. The apical membrane was distorted, and intercellular boundaries were lost (Figure 5 D).

However, renal cortical tissue of recovery group (group III) showed most of changes noticed in the previous group. The podocytes showed indented nucleus and broad fused secondary foot processes. Focal thickening of glomerular basement membrane was seen (Figure 6A).

Proximal convoluted tubules lining epithelium had wide and irregular basal infoldings. The cytoplasm displayed many disoriented mitochondria and vacuoles (Figure 6 B).

Distal convoluted tubules lining epithelium had pyknotic nucleus and vacuolated cytoplasm with many disoriented mitochondria and widening of basal infoldings (Figure 6C).

Conversely, renal cortical tissue of (AD+ Prop) group presented podocytes with euchromatic nuclei and secondary processes were seen wrapping glomerular capillaries. The Glomerular capillaries are lined by endothelial cells and had intact basement membrane (Figure 7 A).

The proximal convoluted tubule has cuboidal epithelial cell lining with euchromatic nucleus and another heterochromatic one, resting on thin defined basement membrane. The epithelial lining has long slim packed luminal microvilli. The cytoplasm exhibited many mitochondria, lysosomes, and vesicles (Figure 7 B).

The distal convoluted tubule has cuboidal epithelial lining with rounded euchromatic nuclei. The epithelium has scarce luminal microvilli and many well defined basal infoldings. The cytoplasm is full of mitochondria and ribosomes. The adjacent cells have apical tight junction (Figure 7 C).

Morphometric results and statistically analysis

Renal corpuscle dimensions

The difference in renal corpuscle diameter between the AD group and the control group was greatly significant ($p \leq 0.001$). In addition, renal corpuscular diameter of the recovery group was substantially smaller than the control group ($p \leq 0.05$). In contrast to the control group, Bowman's space width increased significantly ($p \leq 0.001$) in the AD-treated group. Besides, the recovery group manifested a significant rise ($p \leq 0.05$) in width of Bowman's space as compared to the control group. Propolis intake significantly improved the morphometric findings comprising both corpuscle diameter and width of Bowman's space and there is no significant difference was estimated when compare both (AD+ Prop) and control groups (Histogram 1, Table 6).

Renal tubular measurements

There was a vastly significant rise ($p \leq 0.001$) in the proximal and distal tubular luminal diameter measurements in the AD treated group compared to the control group. Additionally, the recovery group revealed a statistically significant improvement ($p \leq 0.05$) in comparison to the control group. Also, Propolis intake significantly improved the morphometric findings regarding tubular luminal diameter measurements and there is no significant difference was assessed when compare both (AD+ Prop) and control groups (Histogram 2, Table 6).

### Area percent of Mallory's trichrome stained collagen fibers

Compared to the control group, the mean values of collagen fiber area% were significantly greater ($p \leq 0.001$) in the AD group. However, the collagen fiber quantity in recovery group still significantly increased ($p \leq 0.001$). Limited significant amount of collagen fibers was identified in renal cortical interstitial tissue and in glomerular capillaries in the (AD+ Prop) group when compared to the control (Histogram 3, Table 6).

Optical density of P53 immune stained cells

Positive P53 immune marker expression in renal cortical tissue of AD group revealed a highly significance difference ($p \leq 0.001$) as compared to the control group. Positive P53 immune marker expression in the recovery group showed a significant difference ($p \leq 0.05$) as compared to the control group. When comparing the P53 immune expression of the (AD+ Prop) and control groups, there is no discernible change ($p \geq 0.05$). (Histogram 4, Table 6).
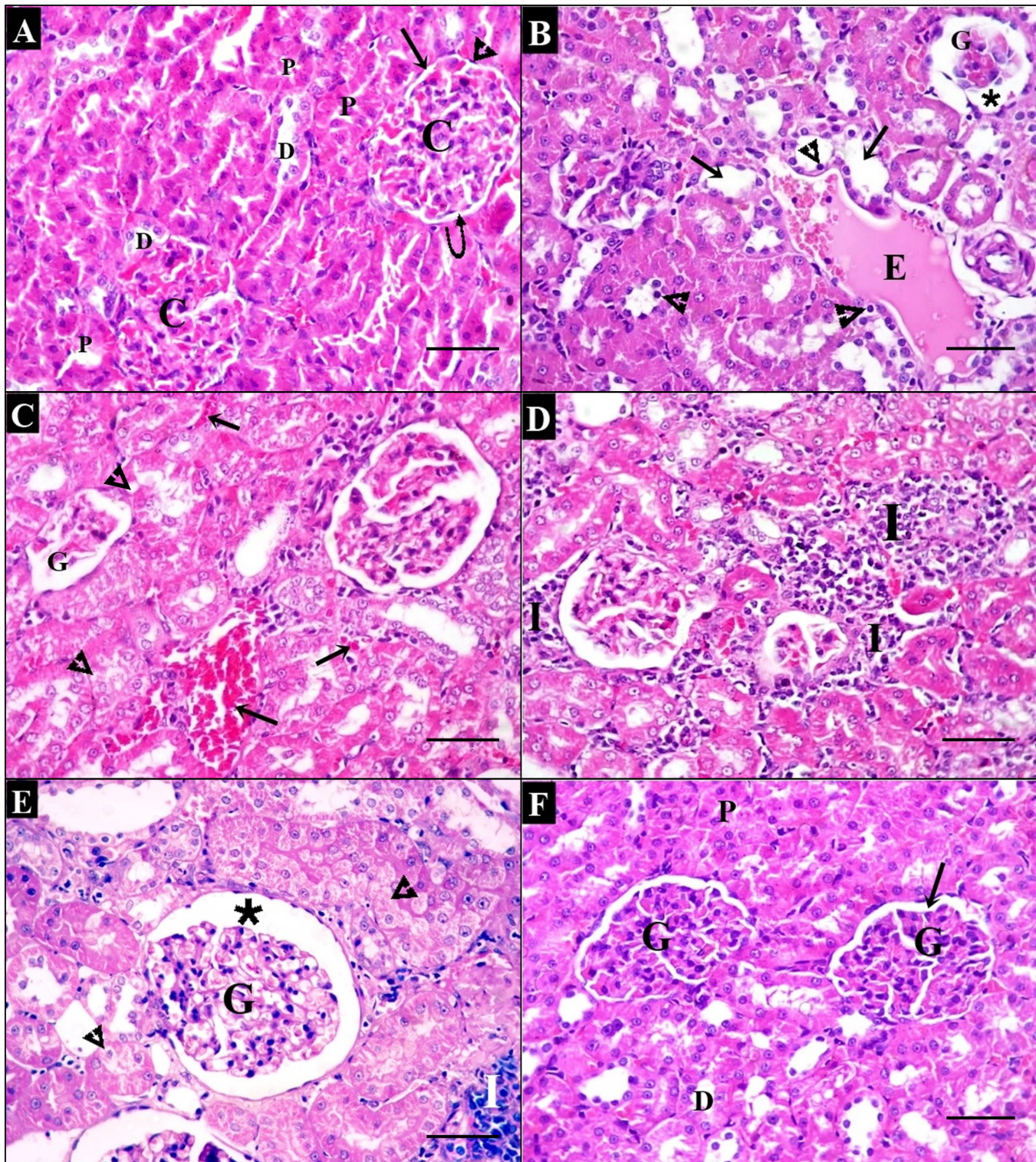
Fig. 1: H&E- stained sections of rat renal cortex (A): The control group showing renal corpuscle (arrow) composed of tuft of capillaries (C) surrounded with parietal layer of Bowman's membrane with its single squamous cell lining (arrow head) with narrow subcapsular space (curved arrow). PCT enclosing narrow lumen (P), lined with cuboidal deeply acidophilic cells with basal rounded nuclei and apical brush border. DCT has wide lumen (D) and lined with less acidophilic cells with central nuclei and less clear brush border. (B): Section from AD group showing massive histological changes in the form of atrophy of the glomerulus (G) with widening of Bowman's space (asterisk). Acidophilic exudate (E) is noticed in renal interstitium. The kidney tubules appear dilated (arrows) and lined by dark stained nuclei (arrowheads). (C): Section from AD group showing interstitial hemorrhage (arrows). Renal tubules appear with vacuolated cytoplasm (arrow heads). Atrophied glomerulus (G) is also seen. (D): Section from AD group showing heavy cellular infiltrate (I). (E): Section from recovery group showing glomerulus with widened Bowman's space (asterisk). Renal tubular cells showing vacuolated cytoplasm (arrow heads). Cellular infiltrate (I) is also noticed. (F): Section from (AD+ Prop) group showing nearly normal picture of the glomerulus (G) with narrow bowman's space (arrow), proximal (P) and distal (D) renal tubules. (A, B, C, D, E, F,   X 400, scale bar 30 μm)
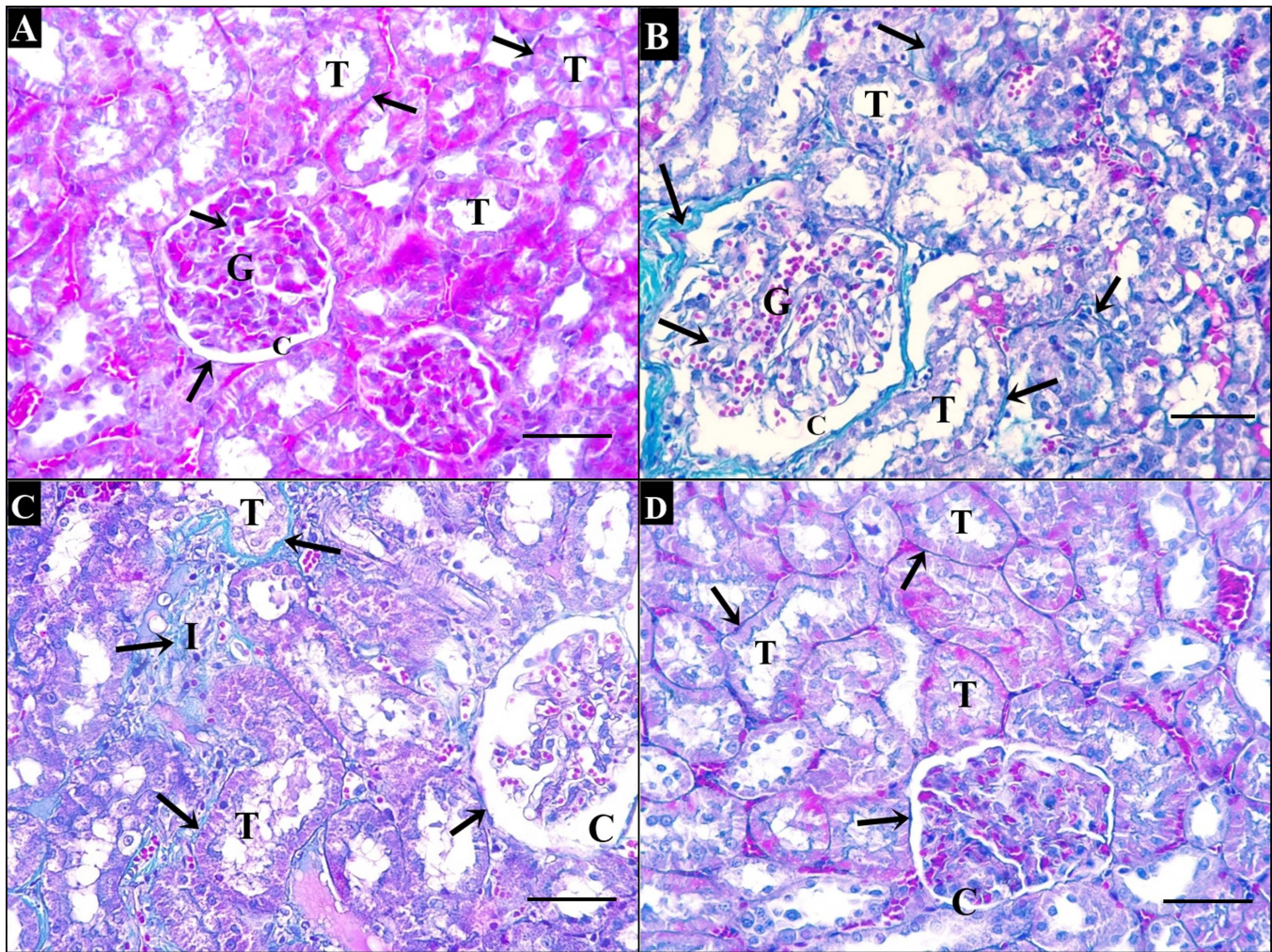
Fig. 2: Mallory trichrome stained sections of rat renal cortex (A): The control group showing few collagen fibers (arrows) around the renal corpuscle (C), glomerular capillaries (G) and renal tubules (T). (B): Section from AD group showing increased collagen fibers (arrows) around the renal corpuscle (C), glomerular capillaries (G) and renal tubules (T). (C): Section from recovery group showing abundant collagen fibers (arrows) in the renal interstitium (I), around renal tubules (T) and renal corpuscle (C). (D): Section from (AD+ Prop) group showing few collagen fibers (arrows) around renal tubules (T) and renal corpuscle (C). (A, B, C, D X 400, scale bar 30 μm)
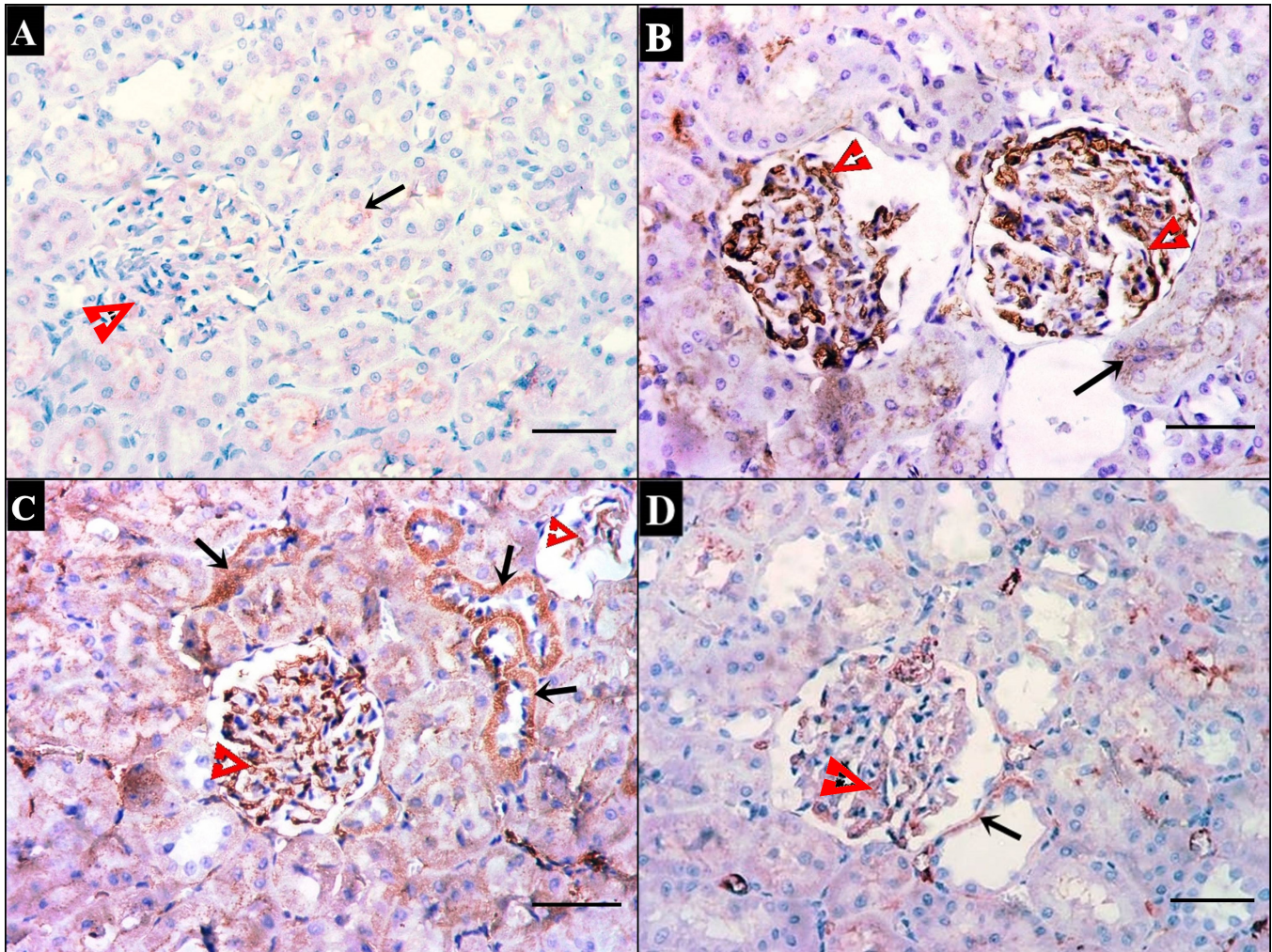
Fig. 3: P53 immunostained sections of rat renal cortex (A): Section from the control group showing faint immunostaining of renal glomerular epithelial cell (arrow head) and tubular cytoplasm (arrow). (B): Sections from AD group displaying intense positive brown immunostaining of renal glomerular epithelial cell (arrow heads) and tubular cytoplasm (arrow). (C): sections from recovery group showing a moderate positive brown immunostaining of renal glomerular epithelial cell (arrow heads) and tubular cytoplasm (arrows). (D): Section from (AD+ Prop) showing minimal positive brown immunostaining of renal glomerular epithelial cell (arrow head) and tubular cytoplasm (arrow). (A, B, C, D X 400, scale bar 30 µm)
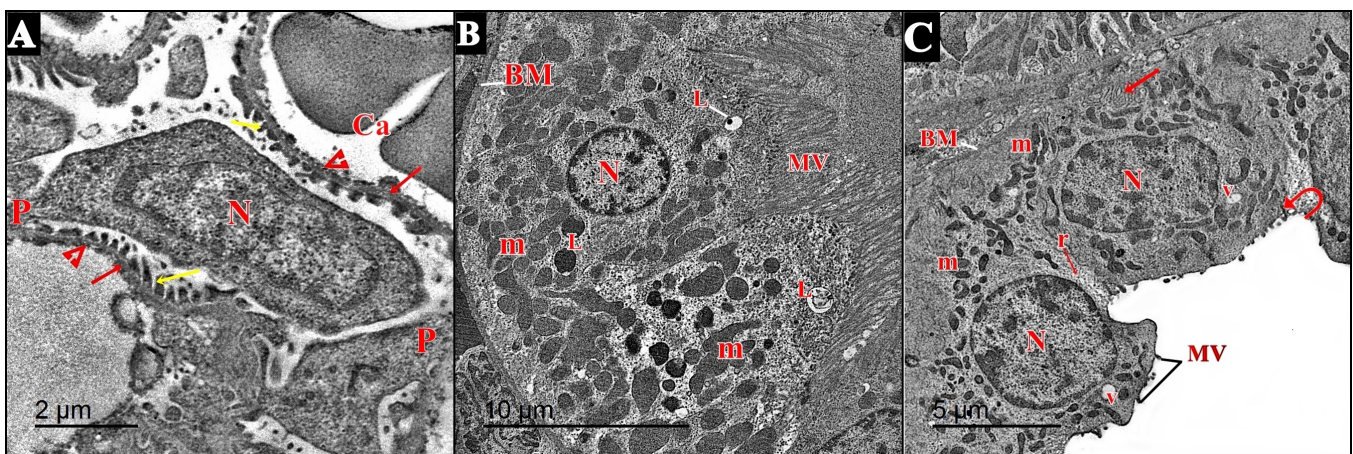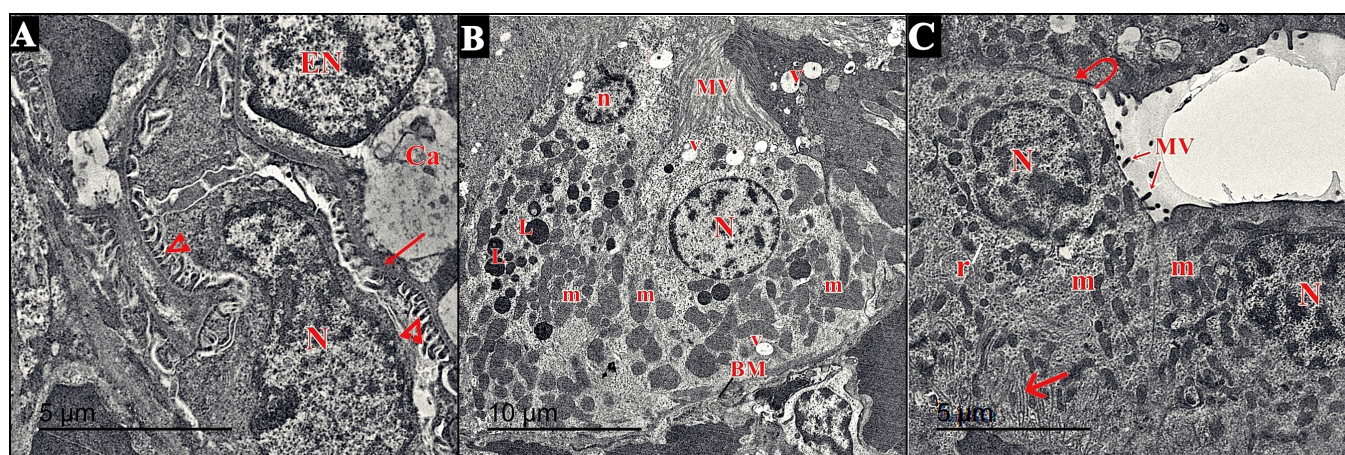

Fig. 4: Transmission electron micrograph of the renal cortex of control rats. (A): Showing renal corpuscle composed of a glomerular capillary (Ca) lined with fenestrated endothelium (arrowhead) and embraced with podocyte with euchromatic nucleus (N). Primary processes (P) are arising from cell body and many secondary processes (yellow arrows) are resting on normal intact smooth basement lamina (red arrows). (B): Proximal convoluted tubular cell showing central euchromatic nucleus (N), resting on well-defined basement membrane (BM). It has long narrow luminal microvilli (MV). Many mitochondria (m) and lysosomes (L) in the cytoplasm. (C): showing distal convoluted tubular cell with central euchromatic nucleus (N), resting on well-defined basement membrane (BM). It has sparse luminal microvilli (MV), basal infoldings (red arrow), elongated mitochondria (m), ribosomes (r) and vesicles (v) in the cytoplasm. Notice tight junction between adjacent cells (curved arrow). (A: Orig. Mag. X 1500 scale bar 2 µm, B X800 scale bar 10 µm, C X1000 scale bar 5 µm)
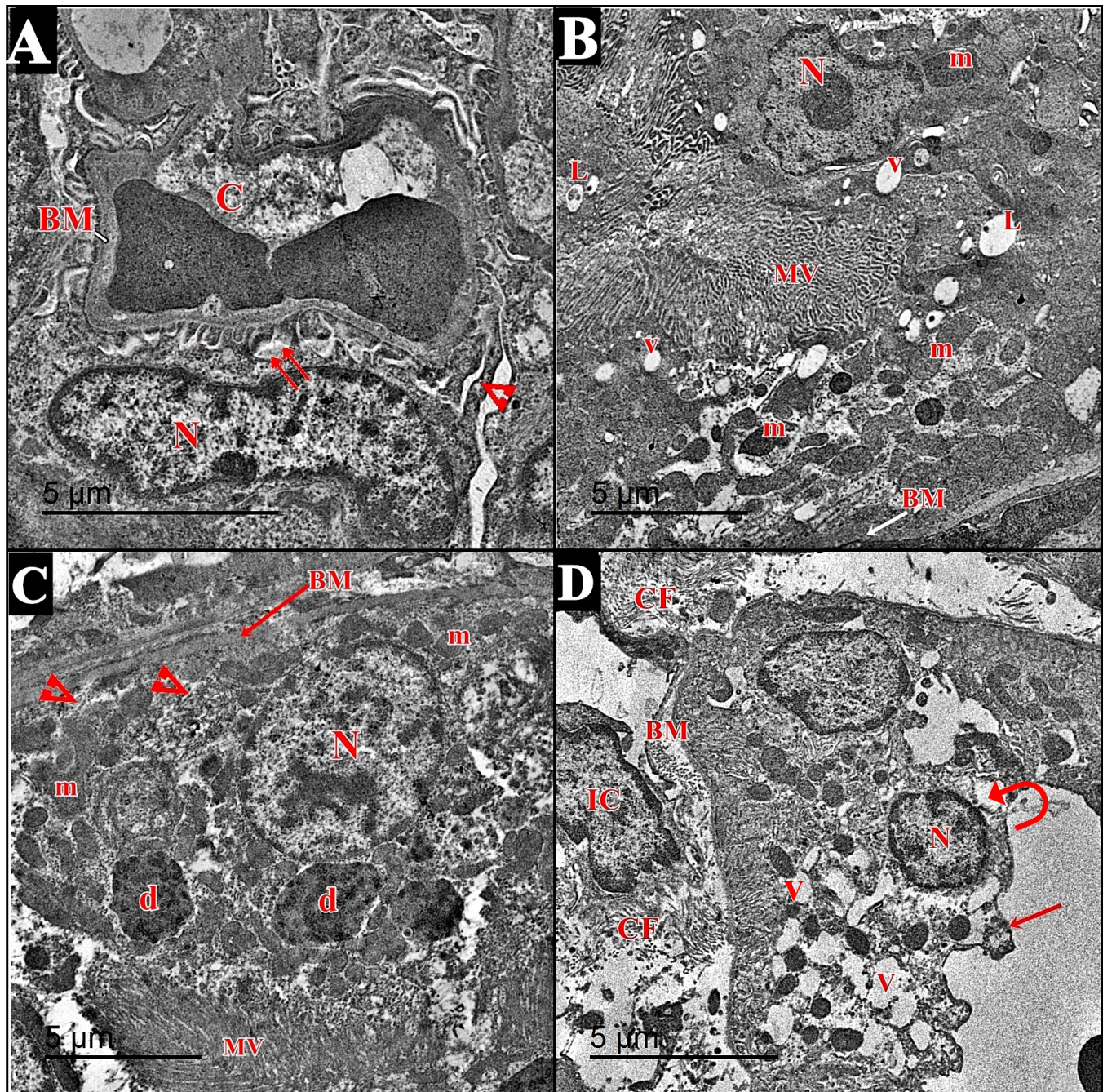
Fig. 5: Transmission electron micrograph of the renal cortex of AD group. (A): Showing a glomerular capillary (C) with irregular thickening of glomerular basement membrane (BM). The podocyte has broad fused secondary processes (double arrow). Primary process (arrow head) is also noticed arising from podocyte. (B-C): Proximal convoluted tubules. In B: showing nucleus (N) with irregular nuclear envelop. Disoriented mitochondria (m), lysosomes (L) and many vacuoles (v) are seen in cytoplasm. Some irregular microvilli (V) and thick basement membrane (BM) are also noticed. (C): showing nucleus (N) with heterochromatic condensation. The cytoplasm is seen disoriented mitochondria (m), electron dense bodies (d). There are few short basal infoldings (arrowheads). Basement membrane (BM) is also noticed. (D): showing distal convoluted tubular cell with small dark stained nucleus (N) and many vacuoles (v) appear in its cytoplasm. The basement membrane (BM) is lost and replaced by many collagen fibers (Cf). Interstitial cell nucleus is seen (IC). The apical cellular membrane is distorted (red arrow) and intercellular boundaries were lost (curved arrow). (A: Orig. Mag. X 1500, B X1000, C X1000, D X1200 scale bar 5 μm)
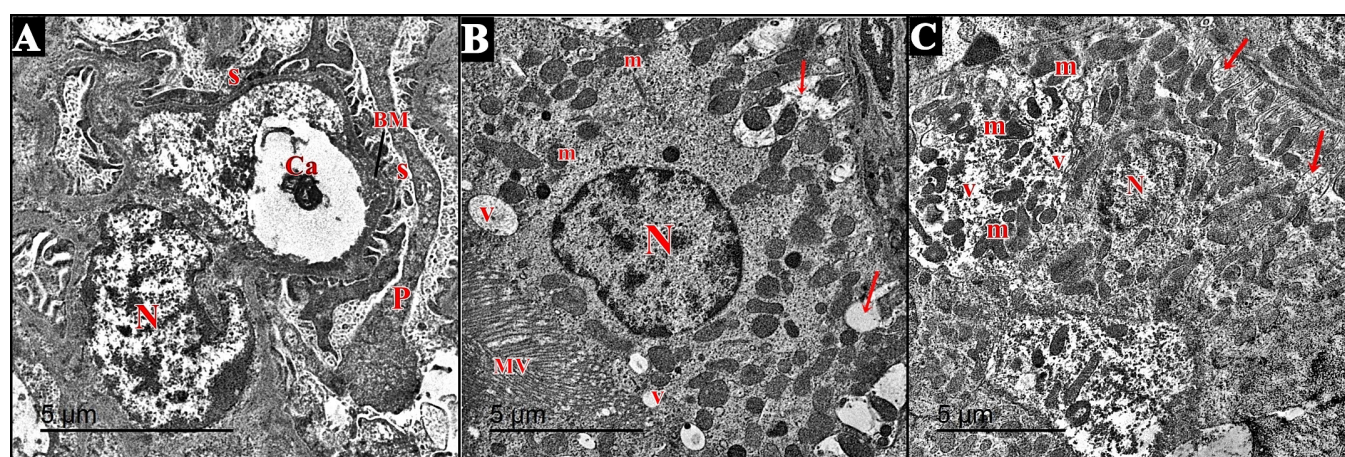
Fig. 6: Transmission electron micrograph of the renal cortex of recovery group rats. (A): Showing the podocyte has indented nucleus (N) and broad fused secondary foot processes (s) are resting on basement membrane with focal area of thickening (BM). In (B): showing proximal convoluted tubular cell with wide irregular basal infoldings (red arrows). The cytoplasm has many disoriented mitochondria (m) and vacuoles (v). (C): Distal convoluted tubular cell showing small nucleus (N) with heterochromatic condensation. Many disoriented mitochondria (m) and vacuoles (v) are seen in the cytoplasm. Notice, the basal infoldings (arrows) are wide. (A: Orig. Mag. X 1500, B X1000, C X1000, scale bar 5 μm)

Fig. 7: Transmission electron micrograph of the renal cortex of (AD+ Prop) group. (A): Showing podocyte with euchromatic nuclei (N) and secondary (arrowheads) foot processes. The glomerular capillary (Ca) is seen lined with endothelial cell (EN) and intact glomerular basement membrane (red arrow) is also noticed. (B): Proximal convoluted tubular cell showing euchromatic nucleus (N) and heterochromatic one (n) in another tubule. It is resting on thin basement membrane (BM) and has many slim packed luminal microvilli (MV). The cytoplasm has many mitochondria (m), lysosomes (L) and many vesicles (v). (C): Distal convoluted tubular cell showing rounded euchromatic nuclei (N). The epithelium has scares luminal microvilli (MV) and many well defined basal infoldings (red arrow). The cytoplasm is full of mitochondria (m) and ribosomes (r). Notice, apical tight junction between adjacent cells (curved arrow). (A: Orig. Mag. X 1500 scale bar 5 μm, B X600 scale bar 10 μm, C X1200 scale bar 5 μm)

Table 2: Body weight, urine volume, serum urea and creatinine levels in the study groups (expressed as mean ± standard deviation).

Parameter	Group I Control (n=6)	Group II AD(n=6)	Group III Recovery (n=6)	Group IV AD+ Prop(n=6)
Body weight change (g)	75 ± 1.22 •, ▲	58 ± 1.35*,♣	48 ± 1.16*,♣	60 ± 10.33•, ▲
Urine volume ml/24h	8.87 ± 0.22•, ▲	30.15 ± 1.72*,♣	28.02 ± 1.32*,♣	11.43 ± 0.12 •, ▲
Serum urea (mg/dl)	26.6 ± 0.15 •, ▲	64.42 ± 1.5*,♣	59.3 ± 1.15 *,♣	27.56 ± 1.12 •, ▲
Serum creatinine (mg/dl)	0.54 ± 1.13 •, ▲	2.59 ± 0.04 *,♣	1.95 ± 1.03 *,♣	0.61 ± 0.12 •, ▲

* Significantly different versus group I ($p \le 0.05$).

• significantly different versus group II ($p \le 0.05$).

▲ significantly different versus group III ($p \le 0.05$).

♣ significantly different from group IV ($p \le 0.05$).

Table 3: serum miRNA-21-5p, miRNA-103a-3p, miRNA-192-5p exepression levels in the study groups:

	Group 1	Group 2	Group 3	Group 4
miRNA-21-5p	1.1±0.3	4.7 ± 0.07	3.1 ± 1.3	2.3 ±0.8
miRNA-103a-3p	0.99±0.1	4.5 ±0.2	3.8 ± 1.5	2.2 ±1.0
miRNA-192-5p	0.97±0.1	3.9 ±0.1	2.9 ±1.3	1.98±1.1

miRNA-21-5p, miRNA-103a-3p, miRNA-192-5p, expression value was significantly higher in group II compared to control group (1) , propolis treated group (4) and recovery group(3). However, we did not find significant changes between groups 1 , 3 and group 4.

Table 4: Renal tissue concentration of GSH-px, SOD, CAT, and MDA among the studied groups (expressed as mean ± standard deviation):

Parameter	Group I Control (n=6)	Group II AD (n=6)	Group III Recovery (n=6)	Group IV AD+ Prop (n=6)
GSH-px (umol/gm)	5.65 ± 1.22•·▲	3.11 ± 0.05*·♦	3.57 ± 0.16*·♦	5.15 ± 10.33•·▲
SOD (u/mg protein)	210.17 ± 0.02•·▲	145.15 ± 0.02*·♦	151.02 ± 0.12*·♦	197.43 ± 0.12•·▲
CAT (u/mg protein)	524.1 ± 0.15•·▲	302.42 ± 0.05*·♦	342.3 ± 0.15*·♦	505.56 ± 1.12•·▲
MDA (nmol/ mg protein)	15.12 ± 1.13•·▲	25.12 ± 0.04*·♦	22.1 ± 0.03*·♦	17.2 ± 0.12•·▲

Glutathione perioxidase (GSH-Px), superoxide dismutase (SOD), catalase (CAT) and malondialdehyde (MDA).
* Significantly different versus group I ($p \leq 0.05$).
• significantly different versus group II ($p \leq 0.05$).
▲ significantly different versus group III ($p \leq 0.05$).
♦ significantly different from group IV ($p \leq 0.05$).
Significant variations were detected in MDA in renal homogenate between the 4 groups Group II showed significantly higher levels of renal MDA while the level decreased in group 3,4 to be closer to the control level in group 4
On the other side, we detected significant differences of antioxidant parameters (SOD & GSH-px &CAT) in renal homogenate, between the studied groups. Adenine decreased the antioxidant parameters (SOD, GSH, and CAT) which were improved by Propolis treatment.

Table 5: Renal tissue concentration of TNF-α, VEGF-A, and MPO among the studied groups

Parameter	Group I Control (n=6)	Group II AD (n=6)	Group III Recovery (n=6)	Group IV AD+ Prop (n=6)
TNF-α (pg/ mg protein)	1.45 ± 1.12•·▲	15.02 ± 1.05*·♦	13.01 ± 0.13*·♦	2.25 ± 0.13•·▲
VEGF-A (pg/mg tissue)	69.07 ± 0.12•·▲	131.05 ± 0.12*·♦	125.12 ± 0.13*·♦	79.13 ± 0.11•·▲
MPO (U/g tissue)	4.85 ± 0.12•·▲	15.22 ± 1.05*·♦	13.11 ± 0.12*·♦	6.27 ± 0.12•·▲

Tumor necrosis factor-alpha (TNF-α), vascular endothelial growth factor-A (VEGF-A) and myeloperoxidase MPO enzyme.
* Significantly different versus group I ($p \leq 0.05$).
• significantly different versus group II ($p \leq 0.05$).
▲ significantly different versus group III ($p \leq 0.05$).
♦ significantly different from group IV ($p \leq 0.05$).
Statistically significant increase was detected in group 2 regarding TNF-α, VEGF-A, and MPO levels while significant decrease occurred in group (4). While in group 3 the levels were still high when compared to control group.

Table 6: Means values of the width of Bowman's space, diameter of renal corpuscle, proximal and distal tubules diameter, area % of collagen fibers and optical density of P53 among the experimental groups

| Parameter	Group I Control	Group II AD	Group III Recovery	Group IV AD+ Prop
Width of Bowman's space (μm)	26.90.1±•·▲	53.20.1±*·♦	50.90.1±*·♦	2٩.91.0±•·▲
Diameter of renal corpuscle (μm)	125.91.0±•·▲	85.81.0±*·♦	90.70.1±*·♦	120.81.0±•·▲
Proximal tubule diameter (μm)	44.9± 1.0•·▲	72.91.0±*·♦	70.70.1±*·♦	4٩.90.2±•·▲
Distal tubule diameter (μm)	89.8± 0.1•·▲	150.7± 0.2*·♦	148.8± 0.01*·♦	١٠٠.1± 0.1•·▲
Area % of collagen fibers	9.870.31±•·▲	26.91.1±*·♦	25.81.2±*·♦	10.30.2±•·▲
Optical density of P53	3.650.12±•·▲	50.92.2±*·♦	48.80.1±*·♦	3.90.1±•·▲

* Significantly different versus group I ($p \leq 0.05$).
• significantly different versus group II ($p \leq 0.05$).
▲ significantly different versus group III ($p \leq 0.05$).
♦ significantly different from group IV ($p \leq 0.05$).
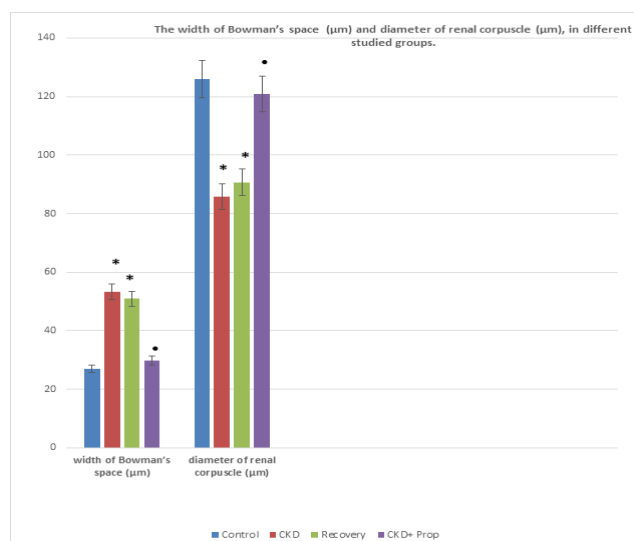
Histogram 1: The width of Bowman's space and diameter of renal corpuscle. in different studied groups. # Significant, ∗ non-significant with control. Data represented as mean ± SD
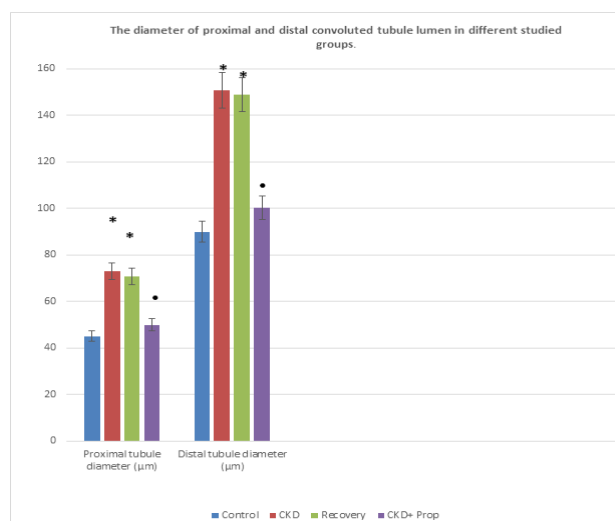
Histogram 2: The diameter of proximal and distal convoluted tubule lumen in different studied groups. # Significant, ∗ non-significant with control. Data represented as mean ± SD
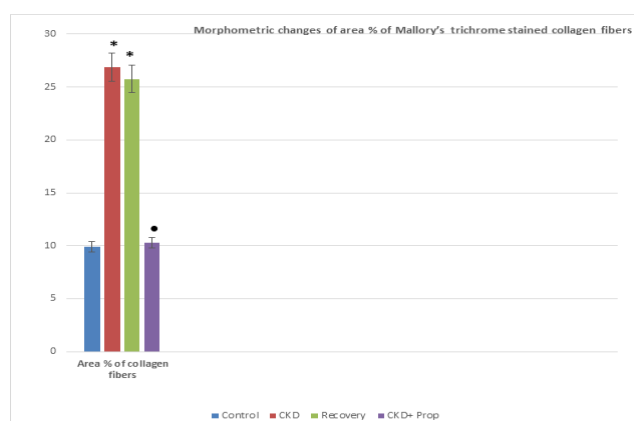
Histogram 3: Morphometric changes of area % of Mallory's trichrome stained collagen fibers and area % of Congo red stained amyloid β protein. ∗ Significant, # non-significant with control. Data represented as mean ± SD.
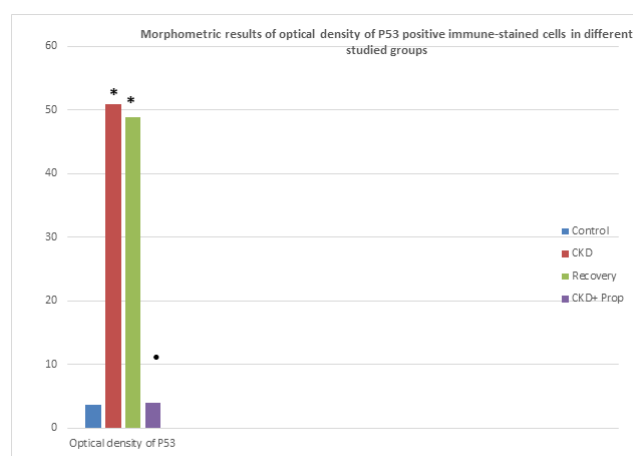
Histogram 4: Morphometric results of optical density of P53 positive immune-stained cells in different studied groups. ∗ Significant, # non-significant with control. Data represented as mean ± SD.

DISCUSSION

Kidney damage is a widespread medical disorder manifested by reduced rate of glomerular filtration, uremia, water, electrolytes, and acid-base imbalance condition. Its mechanism is complex, concerning renal cell necrosis with subsequent inflammatory reaction and accompanying oxidative stress cascade and many other cellular processes[26].

Presently, two experimental means are encountered for CKD induction in animals, specifically the chemical method (by adenine intake in the food) and the surgical method (5/6 renal mass excision). Adenine-induced CKD escapes the possible problems of accompanying surgery to induce CKD. In addition, this method yields more obvious renal changes related to surgical nephrectomy. So, in our study adenine generated CKD in rats was adopted as a disease prototype for the evaluation of the effect of Propolis on CKD[4].

This study was a layout in the direction of disclosing biochemical, cytological and immunohistochemical influences of CKD on the kidney cortical structure and the possible ameliorative effect of Propolis.

By light microscopic examination of AD treated group, glomeruli were shrunken and atrophied with significantly expanded Bowman's space. Some glomerular capillaries endothelia had small darkly stained nuclei. Dilated renal tubules were manifested.

These findings were in accordance with Santos *et al.*[3] who linked adenine induced atrophic glomeruli and renal tubular epithelial degeneration to reactive oxygen species (ROS) development, which shows a critical function in the mechanism of CKD generation. The free oxygen radicals could be accountable for cell membrane lipid peroxidation which causes kidney glomerular and tubular cell death. Hamdy *et al.*[27] added that these adenine effects on renal tissue were hand in hand with biochemical results that showed rise in the MDA level and reduction in the Glutathione perioxidase (GSH-Px). Also, decline of

superoxide dismutase (SOD) and catalase (CAT) levels of adenine group related to the control groups. These levels were reversed after treatment with propolis.

As a sequence of CKD, fibrosis can arise in any renal tissue, for example the glomeruli, tubular interstitial, and renal blood vessels leading to glomerulosclerosis (GS), arteriolosclerosis and tubulointerstitial fibrosis (TIF), correspondingly explaining the degenerative glomerular changes and widening of Bowman's space[28].

Mavrogeorgis *et al*.[29] verified that myofibroblasts (MFBs), are activated under pathological situations, accounting for the extra growth of matrix through development of TIF. Previous research revealed that MFBs can be derived from several cell classes, involving fibroblasts, pericytes, epithelial cells, endothelial cells, bone marrow-resultant fibrocytes and macrophages. Massive production of collagen by stimulated MFBs initiates peritubular capillary pathology, triggering tubular intestinal hypoxia, which shows a fundamental role in the CKD induction and severity.

Renal tubular epithelial hydropic degeneration, renal cortical interstitial acidophilic exudate, congestion, and cellular infiltration could be linked to a significant elevation of several inflammatory activating cytokines and a reduction in inflammatory inhibition cytokines, as was reported by Ali *et al*.[30].

The extremely increased collagen fibers within renal cortical interstitium and renal glomerular capillaries in adenine, was supported by recent findings regarding the up regulation of collagen type VI in cases of renal fibrosis. This kind of collagen is present in the line between the interstitial matrix and basement membrane. CKD as a possible cause of renal fibrosis may up regulate the activity of the proteases enzymes responsible for collagen remodeling and normal amount altering[31].

The Adenine treated group showed intense positive immune expression of p53 in the form of brown coloration of glomerular and tubular epithelial cell cytoplasm. This was described by Overstreet *et al*.[32] as p53 is an essential regulator of podocyte injury accompanying ischemia, diabetes, and obstruction. Fighting P53 is a desirable objective for overcoming advanced renal injuries of various pathologies. Additionally, the same research exposes that TGF-β1, a pro-fibrotic cytokine, facilitates fibrosis despite the preliminary contributing damage, and operates p53 as an important mechanism of fibrotic gene activation. Also, Liu *et al*.[33] discovered the link between renal hypoxia and associated p53 elevation which has a profibrotic effect.

Remarkably, RNS (reactive nitrogen species)/ROS disturbs the mitochondrial membrane potential which encourages the mitochondrial mechanism of apoptosis. In mammals, there is a governing communication between the representation of p21 and p53 as p21 is absolutely stimulated by p53 and it has a crucial mediator function in the p53-tempted apoptosis. The p21 also has a fundamental

function as a motivator of apoptosis through whichever triggering the pro- apoptotic proteins or restraining the anti- apoptotic ones[34].

The electron microscopic findings of the adenine group displayed many histological alterations that support light microscopic findings regarding the massively increased glomerular basement membrane (GBM) thickness. Podocytes are the prime regulator of GBM synthesis, any chronic pathological renal condition alters the basement membrane's accurate steady function via destroying the mechanisms of its maintenance. CKD passively affects renal podocytes leading to abnormal synthesis of GBM matrix components, involving type IV collagen, nidogen and laminin cross linking, GBM becomes more and more disassembled, with resulting barrier role collapse, indicating pathological disorder progression[35].

In our work, the podocytes appeared with broad fused secondary feet processes. This was clarified by Haruhara *et al*.[36] as glomerular tuft decompensatory hypertrophy is a susceptible hypothesis in CKD. The exhaustion of podocytes is an essential influence for the origin and development of glomerulosclerosis and albuminuria. Consequently, podocyte parameters, involving the number, extent, and dimensions, are worthy indicators concerned in the progress and extension of CKD.

Darkly stained irregular nuclei of tubular epithelium, cytoplasmic vacuolations, asymmetrical microvilli, missing intercellular borders and basement membrane with compensatory collagen fibers replacement; all were observed in our research. It was found that the selective damage of tubules is sufficient to induce fibrosis, inflammatory reactions, and capillary damage that justified CKD signs[37]. These changes could be linked to caspases activation which is a crucial pathway that advances to apoptosis in multiple cell types, including tubular cells[38].

The cytoplasmic vacuoles might be empty spaces of damaged mitochondria as explained by Yan *et al*.[39]. They stated that miR-214 induction advocated mitochondrial fragmentation due to disruption of mitochondrial fission-fusion dynamics, which is a significant pathogenic consequence in kidney tubular damage and apoptosis equally in acute plus chronic kidney diseases.

Adenine associated renal injury results from the generation of ROS and RNS as an outcome of large mitochondria content of the kidney's proximal tubular cells. So, it is most exposed to RNS and ROS accompanied renal cells injury. Surprisingly, the kidney is a vulnerable tissue to ROS/RNS-tempted lipids peroxidation and oxidative damage due to the huge amount of polyunsaturated fatty acids. Therefore, the role of ROS is to interact with NO to produce peroxynitrite and accordingly provoke the membranes damage[34].

Diverse reasons, such as hypoxia, oxidative damage, and toxic injury negatively influence renal cells and endanger their existence. Lysosomes contribute to the

albumin management inside the podocytes. Slowdown of lysosomal turnover can raise albumin molecules, worsening podocyte damage and glomerulosclerosis. Diminished lysosomal turnover results in intracellular collection of harmed organelles inside cells[40]. Regular lysosomal activity shows a basic function in influencing the movement of macrophages, consequently improving renal damage[41].

Our histological and immunohistochemical findings revealed marked preservation of normal renal cortical architecture with administration of Propolis in (AD+ Prop) group. We choose Propolis as a possible ameliorative substance in CKD because it was declared in the earlier studies that propolis has a beneficial role in medicines manufactured to cure several chronic illnesses, mainly autoimmune illnesses, gynecological diseases, burns, diabetes complications, injuries, neurodegenerative, gastrointestinal, respiratory, cardiovascular illnesses, microbial infections, tumor, antioxidant roles, and COVID-19[42].

Recently, Propolis was explored for its possible activity concerning restoring renal tissue damage and restoring regular renal function in CKD[43].

These histological results went hand in hand with the biochemical results that cleared marked improvement of antioxidant enzymes levels also decline of MDA level after administration of propolis, confirming its role as antioxidant.

Compared to honey, propolis contains an excessive quantity of minerals, for example calcium, phenols for example pinobanksin-3-oacetate, and flavonoids plus a strong antioxidant property. It was revealed that phenolic compounds both with flavonoids materials ameliorate kidney vascular sclerosis and inflammatory reactions[10].

Silveira 17. found that propolis could diminish the generation of the pro-inflammatory markers; interleukin IL-12, both with interferon IFN-γ and interleukin IL-1β in cell culture, in addition to significantly reduced the enhancement of transcription mediators involved in inflammatory cascade associated with lipopolysaccharide (LPS). It also decreased pulmonary and renal apoptosis and protected the renal mitochondria. Propolis also has anticancer, antidiabetic, and longevity-extending effects[44].

Focak *et al.*[45] added another mechanism of action of Propolis to protect kidneys and reduce oxidative stress by regulating eNOS and heme-oxygenase. The improvement in kidney architecture was reflected in kidney function as a remarkable decline of serum urea and creatinine in propolis treated group along with urine volume that return nearly to normal as in control group.

In our study miRNA were used as advanced biomarkers for kidney function evaluation[46]. These miRNAs are minute non-coding RNA parts about 22 nucleotides length which play role in gene modification of mRNAs leading to translational suppression or mRNA degradation respectively so, they can affect the appearance of many proteins and are associated with different procedures like cell production, cell death, and cell diversion[47].

We used Real-time quantitative polymerase-chain reaction (RT-QPCR) to evaluate the appearance amounts of miRNA-21-5p, miRNA-103a-3p, miRNA-192-5p, in serum. Our results revealed a significant rise in their amounts in CKD group in comparison to control group. These levels were decreased after treatment with propolis as shown in the results.

Our results agreed with Lu *et al.*[48] who discussed the function of miR-103a-3p in angiotensin-II- experimentally induced renal inflammatory reaction and sclerosis. He found that miR-103a-3p levels were significantly raised in patients' urine and sera in cases of hypertensive nephropathy. These effects were mediated through SNRK (SNF-related serine/threonine-protein kinase), that acts as a target of miR-103a-3p.

Another important miR, implied in the pathogenesis of renal disease is miR-192-5p. that had agreat role in fibrosis through reducing ZEB1/2 expression and so increasing mesangial cells collagen synthesis[49].

Putta *et al.*[50] proved that in diabetic mice kidney, reported that downregulation of miR-192-5p tremendously amplified ZEB1/2 synthesis in diabetic mice kidney, whereas diminishing the synthesis of TGF- β1, fibronectin both with collagen, led to less renal scelerosis and less renal failure.

It was noticed also a high amount of miR-21-5p in kidney or serum of diabetic nephropathy in both human and rodents[51] This increased expression was associated with tubular fibrosis, renal damage, with decreased eGFR[52]. Moreover, silencing of miR-21-5p improved PPAR/ retinoid X receptor activity, that acted as defense versus TGF- β1 encouraged fibrous and inflammatory reactions in glomeruli and interstitial cells[53].

CONCLUSION

Phytochemical properties of propolis concentrate presented the existence of numerous biological antioxidants fitting to diverse organic derivatives: phenolics, flavanols, and minerals. All could remain reliable on behalf of the recorded efficiency of propolis concentrate in keeping biological appearances and enzymatic performances of kidney tissue from alterations produced by CKD. Inclusively, daily intake of propolis could provide hopeful protective effects on renal functions. Extra research would have to estimate and explain the accurate process by which these extract, feasibly phenolic combinations, recover CKD oxidative stress and renal damages.

CONFLICT OF INTERESTS

There are no conflicts of interest.

REFERENCES

1. Kovesdy CP. Epidemiology of chronic kidney disease: an update 2022. Kidney Int Suppl (2011) (2022) 12(1):7-11. Doi: 10.1016/j.kisu.2021.11.003. Epub 2022 Mar 18. PMID: 35529086; PMCID: PMC9073222.

2. Bikbov B, Purcell CA, Levey AS, Smith M, Abdoli A, Abebe M, Adebayo OM, Afarideh M, *et al*. Global, regional, and national burden of chronic kidney disease, 1990–2017: a systematic analysis for the global burden of disease study 2017. Lancet (2020) 395 (10225):709–733. DOI:https://doi.org/10.1016/S0140-6736(20)30045-3

3. Santos DIF, Sheriff S, Amlal S, Ahmed RPH, Thakar CV, Amlal H. Adenine acts in the kidney as a signaling factor and causes salt- and water-losing nephropathy: early mechanism of adenine-induced renal injury. Am J Physiol Renal Physiol. (2019) 1; 316(4): F743-F757. Doi: 10.1152/ajprenal.00142.2018. Epub 2019 Jan 9. PMID: 30623725; PMCID: PMC6483032.

4. Kim K, Anderson EM, Thome T, Lu G, Salyers ZR, Cort TA, O'Malley KA, Scali ST, Ryan TE. Skeletal myopathy in CKD: a comparison of adenine-induced nephropathy and 5/6 nephrectomy models in mice. Am J Physiol Renal Physiol. (2021 Jul 1)321(1): F106-F11. Doi: 10.1152/ajprenal.00117.2021. Epub 2021 Jun 14. PMID: 34121452; PMCID: PMC8321803.

5. Khan MA, Nag P, Grivei A, *et al*. Adenine overload induces ferroptosis in human primary proximal tubular epithelial cells. Cell Death Dis. (2022) 13, 104. DOI: https://doi.org/10.1038/s41419-022-04527-z

6. Silveira, MAD, Teles, F, Berretta AA, *et al*. Effects of Brazilian green propolis on proteinuria and renal function in patients with chronic kidney disease: a randomized, double-blind, placebo-controlled trial. BMC Nephrol. (2019) 20, 140. Doi: 10.1186/s12882-019-1337-7. PMID: 31023272; PMCID: PMC6485062.

7. Geyikoglu F, Koc K, Colak S, Erol HS, Cerig S, Yardimci BK, Cakmak O, Dortbudak MB, Eser G, Aysin F, Ozek NS, Yildirim S. Propolis and Its Combination with Boric Acid Protect Against Ischemia/Reperfusion-Induced Acute Kidney Injury by Inhibiting Oxidative Stress, Inflammation, DNA Damage, and Apoptosis in Rats. Biol Trace Elem Res. (2019) 192(2):214-221. Doi: 10.1007/s12011-019-1649-2. Epub 2019 Feb 19. PMID: 30783919.

8. Okail HA, Ibrahim AS and Badr AH. The protective effect of propolis against aluminum chloride-induced hepatorenal toxicity in albino rats. JoBAZ. (2020); 81, 34. DOI: https://doi.org/10.1186/s41936-020-00169-9

9. Laaroussi H, Santos P F, Genisheva Z, Bakour M, Ousaaid D, Teixeira JA, Lyoussi B. Unraveling the chemical composition, antioxidant, α-amylase and α-glucosidase inhibition of Moroccan propolis, Food Bioscience, (2021) 42:101160. DOI: 10.1016/j.fbio.2021.101160

10. Touzani S, Al-Waili N, Imtara H, Aboulghazi A, Hammas N, Falcão S, Boas MV, Arabi IE, Al-Waili W, Lyoussi B. Arbutus Unedo Honey and Propolis Ameliorate Acute Kidney Injury, Acute Liver Injury, and Proteinuria via Hypoglycemic and Antioxidant Activity in Streptozotocin-Treated Rats. Cell Physiol Biochem. (2022 Feb 26) 56(1):66-81. Doi: 10.33594/000000496. PMID: 35218633.

11. Klinkhammer B M, Buchtler S, Djudjaj S, Bouteldja N., Palsson R, Edvardsson VO, Thorsteinsdottir M, Floege J, Mack M, *et al*. Current kidney function parameters overestimate kidney tissue repair in reversible experimental kidney disease. Kidney international. (2022) 102(2); 307–320. Doi: 10.1016/j.kint.2022.02.039. Epub 2022 Apr 26. PMID: 35483527.

12. Nakatsu N, Igarashi Y, Aoshi T, Hamaguchi I, Saito M, Mizukami T, Momose H, Ishii KJ and Yamada H. Isoflurane is a suitable alternative to ether for anesthetizing rats prior to euthanasia for gene expression analysis. J Toxicol Sci. (2017): 42(4):491-497. Doi: 10.2131/jts.42.491. PMID: 28717108.

13. Diwan V, Brown L, Gobe GC. Adenine-induced chronic kidney disease in rats. Nephrology (Carlton). (2018 Jan) 23(1):5-11. Doi: 10.1111/nep.13180. PMID: 29030945.

14. Perera, T., Ranasinghe, S., Alles, N. *et al*. Experimental rat model for acute tubular injury induced by high water hardness and high-water fluoride: efficacy of primary preventive intervention by distilled water administration. BMC Nephrol 21, (2020)103. DOI: https://doi.org/10.1186/s12882-020-01763-3

15. Chavez R, *et al*. Kidney ischaemia reperfusion injury in the rat: the EGTI scoring system as a valid and reliable tool for histological assessment. Journal of Histology and Histopathology, (2016) 3. DOI : http://dx.doi.org/10.7243/2055-091X-3-1

16. Barba C, Benoit B, Bres E, Chanon S, Marchiset AV, Pinteur C , Pesenti S , Glorieux G , Picard C , Fouque D, Soulage CO , Koppe L . A low aromatic amino-acid diet improves renal function and prevents kidney fibrosis in mice with chronic kidney disease. Scientific Reports, (2021) 11 (1): pp.19184. Doi: 10.1038/s41598-021-98718-x. PMID: 34584168; PMCID: PMC8479128.

17. Silveira MAD, Capcha JMC, Sanches TR, Moreira RDS, Garnica MS, Shimizu MH, Berretta A, Teles F, Noronha IL, Andrade L. Green propolis extract attenuates acute kidney injury and lung injury in a rat model of sepsis. Sci Rep. (2021 Mar 15) 11(1):5925. Doi: 10.1038/s41598-021-85124-6. PMID: 33723330; PMCID: PMC7960724.

18. Ohkawa H, Ohishi N, Yagi K. Assay for lipid peroxides in animal tissues by thiobarbituric acid reaction. Anal Biochem. (1979) 95(2):351–358. doi:10.1016/0003-2697(79)90738-3. Doi:10.1016/0003-2697(79)90738-3. doi: 10.1016/0003-2697(79)90738-3. PMID: 36810.

19. Schmittgen TD and Livak KJ. Analyzing real-time PCR data by the comparative C (T) method. Nature Protocols , (2008) 3(6):1101-8. DOI: https://doi.org/10.1038/nprot.2008.73

20. Bancroft J, Layton C Hematoxylin and eosin. In: Suvarna SK, Layton C, Bancroft JD (eds) Theory and practice of histological techniques, Ch. 10 and 11, 7th edn. Churchill Livingstone of Elsevier, Philadelphia, (2013) pp. 172–214. https://doi.org/10.1016/B978-0-7020-4226-3.00010-X

21. Bancroft J and Gamble M. Theory and Practice of Histological Techniques. 7th ed., Churchill Livingston, New York, Edinburgh, London. (2013) Pp: 165-175. E-book ISBN: 978-0-7020-5032-9

22. Nur G, Caylak E, Kilicle PA, Sandayuk S, Celebi OO. Immunohistochemical distribution of Bcl-2 and p53 apoptotic markers in acetamiprid-induced nephrotoxicity. Open Med (Wars). (2022 Nov 21) 17(1):1788-1796. Doi: 10.1515/med-2022-0603

23. Woods A and Stirling J. Electron Microscopy: The preprative techniques. In Bancroft, J. and Gamble, M., (eds): Theory and Practice of Histological Techniques. 5th ed., Churchill Livingston, New York, Edinburgh, London. (2002) Pp: 682-700. E-book ISBN: 0443064350

24. Muralidharan PS, Brigitte H, Petra S, Giovanni P, Roth Eva, François V. Differential Impact of Dietary Branched Chain and Aromatic Amino Acids on Chronic Kidney Disease Progression in Rats. Frontiers in Physiology, (2019)10: article 1460. DOI: 10.3389/fphys.2019.01460

25. Dawson B, and Trapp RG: Basic and clinical biostatistics. 5th ed. New York: McGraw-Hill Education / Medical (2020). E-book ISBN 978-1-260-45536-6

26. Liang RN, Yan DQ, Zhang XP, Chen X, Zhang WH, Jia HL. Kidney Mesenchymal stem cells alleviate cisplatin-induced kidney injury and apoptosis in rats, Tissue and Cell, (2023) 80:101998. DOI: 10.1016/j.tice.2022.101998

27. Hamdy MM, Abdel-Rahman MS, Badary DM, Sabra MS. Effects of furosemide and tadalafil in both conventional and nanoforms against adenine-induced chronic renal failure in rats. Eur J Med Res. (2022 Jul 11) 27(1):117. DOI: 10.1186/s40001-022-00747-3

28. Huang A, Guo G, Yu Y, Yao L. The role of collagen in chronic kidney disease and vascular calcification. J Mol Med (Berl). (2021 Jan) 99(1):75-92. DOI: 10.1007/s00109-020-02014-6

29. Mavrogeorgis E, Mischak H, Latosinska A, Vlahou A, Schanstra JP, Siwy J, Jankowski V, Beige J, Jankowski J. Collagen-Derived Peptides in CKD: A Link to Fibrosis. Toxins (Basel). (2021 Dec 23) 14(1):10. doi: 10.3390/toxins14010010

30. Ali BH, Al Za"abi M, Adham SA, Yasin J, Nemmar A, Schupp N. Therapeutic Effect of Chrysin on Adenine-Induced Chronic Kidney Disease in Rats. Cellular Physiology and Biochemistry (2016 Jan 1) 38 (1): 248–257. DOI: 10.1159/000438626

31. Rasmussen DGK, Boesby L, Nielsen SH, Tepel M, Birot S, Karsdal MA, Kamper AL, Genovese F. Collagen turnover profiles in chronic kidney disease. Scientific Reports. (2019) 9. 10.1038/s41598-019-51905-3. DOI:https://doi.org/10.1038/s41598-019-51905-3

32. Overstreet JM, Gifford CC, Tang J, *et al*. Emerging role of tumor suppressor p53 in acute and chronic kidney diseases. Cell. Mol. Life Sci. (2022) 79: 474. DOI: 10.1007/s00018-022-04505-w

33. Liu L, Zhang P , Bai M , He L , Zhang L , Liu T , Yang Z , Duan M , Liu , Liu BM , Du R , Qian Q , Sun S. P53 upregulated by HIF-1α promotes hypoxia-induced G2/M arrest and renal fibrosis in *vitro* and in *vivo*. Journal of Molecular Cell Biology, (2019 May)11(5): 371–382. DOI: 10.1093/jmcb/mjy042

34. Ibrahim KA, Abdelgaid HA, El-Desouky MA, Fahmi AA, Abdel-Daim MM. Linseed ameliorates renal apoptosis in rat fetuses induced by single or combined exposure to diesel nanoparticles or fenitrothion by inhibiting transcriptional activation of p21/p53 and caspase-3/9 through pro-oxidant stimulus. Environ Toxicol. (2021 May) 36(5):958-974. DOI: 10.1002/tox.23097

35. Marshall CB. Rethinking glomerular basement membrane thickening in diabetic nephropathy: adaptive or pathogenic? Am J Physiol Renal Physiol. (2016 Nov 1) 311(5): F831-F843. DOI: 10.1152/ajprenal.00313.2016

36. Haruhara K, Kanzaki G, Tsuboi N. Nephrons, podocytes, and chronic kidney disease: Strategic antihypertensive therapy for renoprotection. Hypertens Res. (2023) 46: 299–310. DOI: https://doi.org/10.1038/s41440-022-01061-5

37. Liu BC, Tang TT, Lv LL, Lan HY. Renal tubule injury: a driving force toward chronic kidney disease. Kidney Int. (2018 Mar) 93(3):568-579. DOI: 10.1016/j.kint.2017.09.033

38. Barboza JR, Porto ML, de Almeida LS, Freitas FPS, Vasquez EC, *et al*. Probiotic Kefir Prevents Renal IschemiaReperfusion Injury through Reduced Oxidative Stress and Apoptosis in Wistar Rats. J Urol Ren Dis. (2020) 05: 1178. DOI: 10.29011/25757903.001178

39. Yan Y, Ma Z, Zhu J, Zeng M, Liu H, Dong Z. miR-214 represses mitofusin-2 to promote renal tubular apoptosis in ischemic acute kidney injury.American Journal of Physiology-Renal Physiology, (2020) 318:4, F878-F887. doi: 10.1152/ajprenal.00567.2019

40. Zheng HJ, Zhang X, Guo J, Zhang W, Ai S, Zhang F, Wang Y, Liu WJ. Lysosomal dysfunction-induced autophagic stress in diabetic kidney disease. J Cell Mol Med. (2020 Aug)24(15):8276-8290. doi: 10.1111/jcmm.15301

41. Wu M, Zhang M, Zhang Y. *et al*. Relationship between lysosomal dyshomeostasis and progression of diabetic kidney disease. Cell Death Dis. (2021) 12, 958. doi.org/10.1038/s41419-021-04271-w

42. Zullkiflee N, Taha H, Usman A. Propolis: Its Role and Efficacy in Human Health and Diseases. Molecules. (2022 Sep 19)27(18):6120. doi.org/10.3390/molecules27186120

43. Chavda VP, Chaudhari AZ, Teli D, Balar P, Vora L. Propolis and Their Active Constituents for Chronic Diseases. Biomedicines. (2023 Jan 18)11(2):259. doi.org/10.3390/biomedicines11020259

44. Yañez N R, Yañez CRR, Molina GP, Catalá CFM, Cruz ARM, Yañez ON. Biomedical Properties of Propolis on Diverse Chronic Diseases and Its Potential Applications and Health Benefits. Nutrients. (2020 Dec 29)13(1):78. doi: 10.3390/nu13010078

45. Focak M and Suljevic D. Ameliorative Effects of Propolis and Royal Jelly against CCl4 -Induced Hepatotoxicity and Nephrotoxicity in Wistar Rats. Chem Biodivers. (2023 Jan) 20(1): e202200948. DOI:10.1002/cbdv.202200948

46. Wang M, Yu F, Ding H, Wang Y, Li P, Wang K. Emerging Function and Clinical Values of Exosomal MicroRNAs in Cancer. Mol. Ther. Nucleic Acids, (2019) 16: 791–804. DOI: 10.1016/j.omtn.2019.04.027

47. O'Brien J, Hayder H, Zayed Y, Peng C. Overview of microRNA biogenesis, mechanisms of actions and circulation. Front Endocrinol (Lausanne). (2018) 9:402. doi.org/10.3389/fendo.2018.00402

48. Lu Q, Ma Z, Ding Y, Bedarida T, Chen L, Xie Z, Song P, Zou MH. Circulating miR-103a-3pcontributes to angiotensin II-induced renal inflammation and fibrosis via a SNRK/NF-kappaB/p65 regulatory axis. Nat. Commun. (2019) 10: 2145. DOI: 10.1038/s41467-019-10116-0

49. Kato M, Zhang J, Wang M, Lanting L, Yuan H, Rossi JJ, Natarajan R. MicroRNA-192 in diabetic kidney glomeruli and its function in TGF-beta-induced collagen expression via inhibition of E-box repressors. Proc. Natl. Acad. Sci. USA.(2007) 104: 3432–3437. DOI: 10.1073/pnas.0611192104

50. Putta S, Lanting L, Sun G, Lawson G, Kato M, Natarajan R. Inhibiting microRNA-192 ameliorates renal fibrosis in diabetic nephropathy. J. Am. Soc. Nephrol. (2012)23: 458–469. DOI: 10.1681/ASN.2011050485

51. Chen X, Zhao L, Xing Y, Lin B. Down-regulation of microRNA-21 reduces inflammation and podocyte apoptosis in diabetic nephropathy by relieving the repression of TIMP3 expression. Biomed. Pharmacother. (2018) 108: 7–14. DOI: 10.1016/j.biopha.2018.09.007

52. Kolling M, Kaucsar T, Schauerte C, Hubner A, Dettling A, Park JK, Busch M, Wulff X, Meier M, Scherf K. *et al*. Therapeutic miR-21 Silencing Ameliorates Diabetic Kidney Disease in Mice. Mol. Ther. J. Am. Soc. Gene Ther. (2017)25: 165–180. DOI: 10.1016/j.ymthe.2016.08.001

53. Gomez IG, MacKenna DA, Johnson BG, Kaimal V, Roach A, Ren S, Nakagawa N, Xin C, Newitt R, Pandya S. *et al*. Anti-microRNA-21 oligonucleotides prevent Alport nephropathy progression by stimulating metabolic pathways. J. Clin. Investig. (2014) 125, 141–156. doi: 10.1172/JCI75852

الملخص العربى

دراسة هستولوجية و هستوكيميائية مناعية على التأثير التحسيني المحتمل للبروبوليس في مرض الكلى المزمن المستحدث تجريبيا بالأدينين في ذكور الجرذان البيضاء البالغة

نادية العقباوي¹، هبه محمد النجرس¹‚²، عبير علي عبدالرحمن³، ابتهال زيد حسن¹

قسم الأنسجة الطبية وبيولوجيا الخلية – كلية الطب ـ ¹جامعة الزقازيق ـ ²جامعة بدر – القاهرة

³قسم الكيمياء الحيوية الطبية والبيولوجيا الجزئية – كلية الطب ـجامعة الزقازيق

المقدمة: يعد مرض الكلى المزمن مصدر قلق عالمي على الصحة العامة. و يلعب الالتهاب والإجهاد التأكسدي دورًا في الفيزيولوجيا المرضية لهذا المرض والمضاعفات المرتبطة به، واللتي تتشابه في الانسان والحيوان. تهدف هذه الدراسة إلى اكتشاف أساليب علاجية جديدة لمرض الكلى المزمن.

الهدف: تهدف هذه الدراسة إلى دراسة التأثيرات التحسينية للبروبوليس في النموذج المستحدث تجريبيا بالأدينين لمرض الكلى المزمن.

مواد وطرق البحث: تم تخصيص أربعة وعشرين فأرًا وتقسيمهم إلى أربع مجموعات متساوية على النحو التالي: المجموعة الضابطة، مجموعة الأدينين: تلقت المجموعة ٢٠٠ ملغم من الأدينين / كغم / يوم عن طريق الفم لمدة٢٨يومًا لأستحداث مرض الكلى المزمن، (مجموعة الاستشفاء) تلقت الأدينين كالمجموعة السابقة ثم تركت دون علاج لمدة ١٤ يومًا أخرى . (المجموعة المعالجة بالبروبوليس): تلقت البروبوليس بجرعة ١٠٠ ملجم/كجم وزن الجسم/يوم بالإضافة إلى الأدنين لمدة ٢٨ يوم. وفي نهاية التجربة تم قياس وزن الجسم ووزن الكلى لجميع المجموعات. كما تم أخذ عينات دم لقياس نسبة اليوريا والكيرياتينين في السيرم . وتم قياس دلالات الإجهاد التأكسدي واختبارات وظائف الكلى ومستويات miRNA-21-5p وmiRNA-103a-3pوmiRNA-192-5p . كما تم إجراء صبغ مناعي كيميائي لعامل نخر الورم α وقياس التغيرات المرضية في أنسجة الكلى.

النتائج: عدل البروبوليس التغيرات الدينـاميكية الدموية الكلوية بأمان وقلل فقدان وزن الجسم وحجم البول الناجم عن مرض الكلى المزمن. بالإضافة إلى ذلك، فقد عدل الدلالات الحيوية للإجهاد التأكسدي واختبارات وظائف الكلى بأمان. كما تم توثيق انخفاض كبير في التصبغ المناعي P53 و ظهر تضاؤل كبيرفي التغيرات النسيجية المرضية الناجمة عن مرض الكلى المزمن.

الخلاصة: قد يكون للبروبوليس دورًا واعدًا في الحفاظ على بنية ووظيفة أنسجة الكلى في مرض الكلى المزمن المسحتدث بالأدنين ، مما يجعله مكملاً مطلوبا.